Effects of different closures for thickness diffusivity

Carsten Eden [a,*], Markus Jochum [b], Gokhan Danabasoglu [b]

[a] IFM-GEOMAR, Düsternbrooker Weg 20, 24105 Kiel, Germany
[b] NCAR, 1850 Table Mesa Drive, Boulder, Colorado 80305, USA

ARTICLE INFO

ABSTRACT

The effects of spatial variations of the thickness diffusivity (K) appropriate to the parameterisation of [Gent, P.R. and McWilliams, J.C., 1990. Isopycnal mixing in ocean circulation models. J. Phys. Oceanogr., 20, 150–155.] are assessed in a coarse resolution global ocean general circulation model. Simulations using three closures yielding different lateral and/or vertical variations in K are compared with a simulation using a constant value. Although the effects of changing K are in general small and all simulations remain biased compared to observations, we find systematic local sensitivities of the simulated circulation on K. In particular, increasing K near the surface in the tropical ocean lifts the depth of the equatorial thermocline, the strength of the Antarctic Circumpolar Current decreases while the subpolar and subtropical gyre transports in the North Atlantic increase by increasing K locally. We also find that the lateral and vertical structure of K given by a recently proposed closure reduces the negative temperature biases in the western North Atlantic by adjusting the pathways of the Gulf Stream and the North Atlantic Current to a more realistic position.

1. Introduction

In many state-of-the-art, non-eddy-resolving ocean models the so-called thickness diffusivity K appropriate to the Gent and McWilliams (1990) (GM) parameterisation is used. This lateral diffusivity is meant to account for the advective effects of the turbulent lateral mixing by meso-scale eddies. In the GM parameterisation, the value of K has to be specified and was chosen in the past as a constant value of $\mathcal{O}(1000 \text{ m}^2/\text{s})$. Modern ocean models, however, are beginning to incorporate spatially varying thickness diffusivities (Griffies et al., 2005; Danabasoglu and Marshall, 2007). It is the aim of this study to compare a representative selection of such closures for K in a global ocean model and to document their impacts on the simulated circulation and watermass characteristics. In particular, we consider four different choices for the thickness diffusivity:

- $K = 800 \text{ m}^2/\text{s}$, i.e. a constant value (experiment CONST);
- $K(x,y,t)$ as suggested by Visbeck et al. (1997), i.e. $K = \alpha L^2 \bar{\sigma}$ where $\bar{\sigma}$ is the Eady growth rate averaged over the main thermocline, L an eddy length scale and α a tuning parameter (experiment VMHS);
- $K(x,y,z,t)$ as suggested by Danabasoglu and Marshall (2007) dependent on the local stability frequency (N), i.e. $K = K_0 N^2 N_{\text{ref}}^{-2}$ with the parameters K_0 and N_{ref} as specified below (experiment NSQR);

- $K(x,y,z,t)$ dependent on an eddy length scale and time scale as suggested by Eden and Greatbatch (2008b), i.e. $K = cL^2 \sigma$ where σ is the local Eady growth rate and L the minimum of Rossby radius and Rhines scale (experiment EG).

In CONST, the thickness diffusivity K shows no spatial or temporal variation (except for a tapering procedure) and can be considered as the zeroth order choice. This choice is often used due to the lack of knowledge about a physically meaningful spatial dependency of K. In a first step beyond a constant value, Visbeck et al. (1997) suggested to use a mixing length approach, first proposed for geophysical applications by Green (1970) and Stone (1972). Visbeck et al. (1997) chose the inverse Eady growth rate (σ) as a time scale and the maximum of the local Rossby radius, grid spacing or the width of the baroclinic zone (of the region of interest) as the eddy length scale. They also assumed a vertically constant K.

On the other hand, it is often proposed that K should also have a vertically varying structure. Danabasoglu and McWilliams (1995) and Jochum (1997) proposed prescribed exponentially varying vertical profiles for K. Ferreira et al. (2005) estimated the optimal value of K in a non-eddy-resolving model simulation using an adjoint technique, while Eden et al. (2007) and Eden (2006) diagnosed K directly from results of high-resolution models. In these studies significant horizontal and also vertical variations of K were found, with magnitudes ranging from zero to more than 5000 m²/s, consistent with previous estimates of eddy diffusivity from observations and models (Rix and Willebrand, 1996; Ledwell et al., 1998; Stammer, 1998; Bryan et al., 1999; Treguier, 1999; Nakamura and Chao, 2000; Roberts and Marshall, 2000; Drijfhout

and Hazeleger, 2001; Solovev et al., 2002; Zhurbas and Oh, 2004; Marshall et al., in press). In general all these studies, and in particular Ferreira et al. (2005) and Eden et al. (2007), also agree in the finding of large K in the upper thermocline and small values below, which motivated Ferreira and Marshall (2006) and later Danabasoglu and Marshall (2007) to investigate the impacts of using K proportional to the square of the buoyancy frequency (N^2) in a model. This choice was motivated by the finding that N^2 shows a similar vertical structure as the diagnosed K in Ferreira et al. (2005), Eden et al. (2007) and Eden (2006). Our experiment NSQR is identical to experiment ITN2 discussed in Danabasoglu and Marshall (2007).

An alternative closure which we consider here (experiment EG) is a simplified version of the parameterisation of Eden and Greatbatch (2008b). It is based on a mixing length approach by Green (1970) and Stone (1972) and a prognostic budget for eddy kinetic energy with parameterised sources (due to baroclinic and barotropic instability), transports and sinks (dissipation). A simplified and localised form of the closure (as used here in experiment EG) was shown to agree in mid-latitudes with the scaling laws of Larichev and Held (1995) and Held and Larichev (1996). We consider this closure here because it combines vertical variations with horizontal ones.

It was found in Eden and Greatbatch (2008b) that the application of this new closure did not change much a North Atlantic model simulation of $\mathcal{O}(1^\circ)$ resolution compared to a simulation using a constant value of K. This result is qualified here since in agreement with Danabasoglu and Marshall (2007) we find indeed certain improvements of a global ocean model simulation of $\mathcal{O}(3^\circ)$ resolution and it is our aim to document these improvements. We also report some systematic model dependencies of the circulation on the value of the thickness diffusivity, such as the strength of the subpolar gyre with impacts on convective activity and ventilation rates of the North Atlantic, and the depth of the equatorial thermocline with potential effects on coupled climate models. The next section will describe the model and the details of the experiments, the third section will discuss the results and the last section provides a summary and a discussion.

2. Numerical experiments

In all experiments, a state-of-the-art coarse-resolution ocean model based on the Parallel Ocean Program of the Los Alamos National Laboratory (Smith and Gent, 2004) is used, which is also the (coarse resolution version) ocean component of the Community Climate System Model (CCSM). It is a global, *z*-level-coordinate model with the grid North Pole displaced into Greenland with nominal 3° horizontal resolution (Yeager et al., 2006).[1] There are 25 vertical levels, monotonically increasing from 8 m near the surface to about 500 m in the abyssal ocean. The surface forcing is given by the normal-year forcing data provided by Large and Yeager (2004) at T62 resolution. There is no active sea ice model. The vertical mixing coefficients are determined using the K-Profile Parameterisation of Large et al. (1994), as modified by Danabasoglu et al. (2006). More details about the model setup can be found in, e.g., Danabasoglu et al. (2008). In the following we only discuss issues relevant for the thickness diffusivity.

In each experiment, a preliminary version of the near-surface eddy flux parameterisation of Ferrari et al. (in press), as implemented by Danabasoglu et al. (2008), is used in the model tracer equations. In this new approach, a transition layer separates the quasi-adiabatic interior where eddy fluxes are oriented along iso-

pycnals from the diabatic, near-surface regions (e.g., the boundary layer) where diapycnal meso-scale fluxes are directed along the ocean surface. In the interior, eddy fluxes are still represented using the isopycnal diffusion tensor (Redi, 1982; Cox, 1987) and the Gent and McWilliams (1990) parameterisation for eddy induced advection with spatially varying identical diffusivities for both (see below). As the surface is approached, the meso-scale eddy fluxes become parallel to the ocean surface, crossing outcropping density surfaces. This behaviour is parameterised using a down-gradient horizontal diffusion with a mixing coefficient of K_H, which has the same value as the interior isopycnal/thickness diffusivity, i.e., K, indicating that the interior and near-surface mixing rates remain the same. A linear combination of horizontal and isopycnally-oriented mixing occurs within the surface diabatic layer. The eddy-induced velocity is parallel to the ocean surface and has no vertical shear within the boundary layer. It must then develop vertical shear within the transition layer to match the interior values. We use the mixed layer depth as defined in Large et al. (1997) to represent the diabatic layer depth in the present simulations. We note that this new scheme eliminates the need for any ad-hoc, near-surface taper functions usually used with the Gent and McWilliams (1990) scheme. Further details of the near-surface eddy parameterisation are given in Danabasoglu et al. (2008).

In the quasi-adiabatic interior, four different choices for the thickness diffusivities are used. We note that in each experiment both thickness and isopycnal diffusivities are modified identically, i.e. they have the same value. This choice is supported by the identical diffusivity tensors for thickness and isopycnal mixing obtained as a result of the adiabatic stochastic theory of tracer transport, e.g. Dukowicz and Greatbatch (1999), and by a recent diagnosis of isopycnal diffusivities using results from a high-resolution model simulation (Eden and Greatbatch, submitted for publication). One often assumes that the choice for the value of isopycnal diffusivity does not effect much the buoyancy (the effect is due to mixing of different watermasses in the presence of a non-linear equation of state) and thus have a negligible effect on the dynamics. We note, however, that ocean model solutions can show sensitivities to various choices of isopycnal diffusivity (Danabasoglu and Marshall, 2007) and that isopycnal diffusivity can play a larger role than one might expect when changes in watermass characteristics become large (Sijp et al., 2006). Although a detailed investigation of the sensitivities of model solutions to isopycnal diffusivity changes is beyond the scope of the present work, we present a brief discussion of this issue when we consider an ideal age tracer because for passive tracers with large gradients on isopycnals the choice of isopycnal diffusivity becomes important.

The main experiments (CONST, VMHS, NSQR and EG) have been integrated for 500 years each. We note that this integration length might be too short for a complete diffusive equilibrium of the ocean model, for which the time scale would be several thousand years. Consequently, in this study we focus on the dynamical effects of the thickness diffusivity, for which the integration length should be sufficient (compare for instance Figs. 2a and 3. of Danabasoglu (2004)). Furthermore, for a longer integration period we do not expect changes in the differences between the four main individual experiments on which we build our conclusions. Note also that the diffusive equilibrium will also depend to a large extent on parameterisation of diapycnal diffusivity and surface forcing, issues which are left aside in the present study. Additional sensitivity experiments are integrated for 100 years each, for which we also expect to obtain the important differences between the experiments during this integration period. In the remainder of this section, a large number of relevant model details are discussed separately for each experiment.

---

[1] Zonal resolution is uniform at 3.6°, but the meridional resolution varies from 0.4° to 0.6° in the subpolar northeast Atlantic and at the equator, respectively, to about 3° in the Southern Hemisphere mid-latitudes and northwest Pacific.

2.1. Experiment CONST

The constant value of $K = 800$ m^2/s in experiment CONST, was found to produce simulations in good agreement with observations in Danabasoglu (2004). We therefore use this value as well here and consider it as the optimal (constant) value for this particular ocean model.

2.2. Experiment VMHS

In experiment VMHS the thickness diffusivity is given by $K = \alpha L^2 \bar{\sigma}$. The mean Eady growth rate $\bar{\sigma} = f \bar{Ri}^{-1/2}$ is calculated from the Richardson number $\bar{Ri} = \overline{N^2 \left| \frac{\partial}{\partial z} \boldsymbol{u}_\mathrm{h} \right|^{-2}}$ averaged between 100 and 2000 m depth and is representative of the Eady growth rate within the main thermocline of the ocean. Here, $\boldsymbol{u}_\mathrm{h}$ denotes the horizontal velocity vector and f the Coriolis parameter. Visbeck et al. (1997) proposed to use as the eddy length scale L the maximum of the local Rossby radius (L_r), the local grid spacing of the model (Δ) and the width of the baroclinic zone (L_BZ), where the latter is defined as the width of the region in which $\bar{\sigma}$ exceeds 10% of the maximum of $\bar{\sigma}$ in that region. Wright (1997) discusses an implementation of the original scheme by Visbeck et al. (1997) in a global coupled model of the British Met Office with $\alpha = 0.015$ (same value as suggested by Visbeck et al. (1997)), with $\bar{\sigma}$ averaged over the upper 2000 m and L_BZ as length scale. Their Fig. 3 shows that over most of the ocean, the simulated K approaches its lower bound (chosen as 300 m^2/s), while only in the Southern Ocean moderately increased values of K can be seen (and some in the Labrador and Irminger Seas) which appears to be inconsistent with the previous estimates of K which show increased values of K in other regions as well (see also Section 3.1).

We decided therefore not to use L_BZ as the length scale. We also found that using only the Rossby radius L_r as length scale in the model yields too low values of K at higher latitudes, or, in turn, too high values in the subtropics (by adjusting the parameter α). Therefore, we decided to use in experiment VMHS $L = \max(\bar{L}_\mathrm{r}, \Delta)$, where Δ denotes the local horizontal grid spacing, $\alpha = 0.13$ and where the local Rossby radius is approximated by $\bar{L}_\mathrm{r} = \bar{N} h_\mathrm{vis} f^{-1}$ with $\bar{N} = (\overline{N^2})^{1/2}$ (the vertical mean is taken over the same depth range h_vis as for $\bar{Ri}$). Furthermore, $\bar{L}_\mathrm{r}$ is replaced from its mid-latitude form to the equatorial Rossby radius near the equator. However, the Eady growth rate and thus K will go to zero near the equator. This is because the closure is based on heuristic considerations relevant for mid-latitude baroclinic instability theory, which becomes inappropriate at the equator. To prevent K from vanishing near the equator, f is replaced with $\sqrt{2\beta c_\mathrm{r}}$ as the relevant equatorial time scale in VMHS near the equator. Here, $\beta = \frac{\partial}{\partial y} f$ and c_r denotes the first baroclinic Rossby wave speed. The resulting diffusivity K is furthermore bounded by 300 m^2/s $\leqslant K \leqslant$ 4000 m^2/s.

Note that the length scale L is important for the parameterisation of Visbeck et al. (1997) and significantly affects the choice of the parameter α. In our version of VMHS, we have tried to reproduce our a priori knowledge of the magnitude and large scale pattern of K as best as we could, but other choices for L could be possible and might produce better results in this respect. We regard experiment VMHS as an example for many other possibilities in the spirit of Visbeck et al. (1997), which, however, have a vertically constant K in common.

2.3. Experiment NSQR

In experiment NSQR, we follow Danabasoglu and Marshall (2007) and set $K_0 = 4000$ m^2/s. The reference value for the stability frequency N_ref is chosen at each horizontal position as the uppermost value of N in the quasi-adiabatic interior layer provided that $N^2 > 0$ there, otherwise, N_{ref} is given by the first $N^2 > 0$ further below. The resulting thickness diffusivity is bounded by $K_0/10 \leqslant K \leqslant K_0$.

2.4. Experiment EG

In experiment EG, the thickness diffusivity is given by $K = cL^2\sigma$. The eddy length scale L is given as the minimum of the Rossby radius L_r and Rhines scale $L_\mathrm{Rhi} = \sqrt{\bar{e}^{1/2}\beta^{-1}}$, where $\bar{e}$ denotes eddy kinetic energy. This choice for L was found to be consistent with independent estimates of eddy length scales from satellite observations (Eden, 2007) and with high-resolution model results (Eden, 2007) and with recent theoretical considerations (Theiss, 2004). L_Rhi is estimated from variables of the coarse resolution model as $L_\mathrm{Rhi} = \sigma/\beta$ (Eden and Greatbatch, 2008b) while L_r is given by $L_\mathrm{r} = \min\left[\frac{c_\mathrm{r}}{|f|}, \sqrt{\frac{c_\mathrm{r}}{2\beta}}\right]$ where c_r denotes the first baroclinic Rossby wave speed, which is calculated approximately following Chelton et al. (1998) by $c_\mathrm{r} \approx \int_{-h}^{0} N/\pi \, dz$, where h denotes the local water depth. The inverse eddy time scale σ was found by Eden and Greatbatch (2008b) as given by $\sigma = |\nabla_h \bar{b}|/N$, which is, by the thermal wind relation, for mid-latitudes identical to the Eady growth rate $\sigma = f \, Ri^{-1/2}$. Here, $Ri = N^2 \left| \frac{\partial}{\partial z} u_\mathrm{h} \right|^{-2}$ denotes the local Richardson number in contrast to a vertically averaged Ri as in VMHS. Note that we have used the latter formulation for Ri using the vertical shear of the horizontal velocity in the model code as before in experiment VMHS.

It is clear that σ has a singularity as $N \to 0$. To prevent this singularity we use $\sigma = f(Ri + \gamma)^{-1/2}$ with $\gamma > 0$ which acts effectively as an upper limit for σ and consequently for K. Note that this approach is motivated by the fact that effective growth rates are replaced by $f(Ri + 1)^{-1/2}$ for baroclinic instability under weak stratification (Stone, 1971, 1972). The effect of γ and the tuning parameter c will be further explored below. They were initially set to $\gamma = 200$ and $c = 2$ in experiment EG. However, note that $Ri \gg 200$ within the thermocline (i.e. roughly between 100 and 800 m depth) except near the surface diabatic layer (and in abyssal, almost unstratified regions), such that the choice of γ for $\sigma = f(Ri + \gamma)^{-1/2}$ is only relevant approaching the mixed layer where the tapering scheme becomes active as well.

Note that using $\sigma = f(Ri + \gamma)^{-1/2}$ in EG, the time scale and thus K goes to zero at the equator, as in experiment VMHS. To prevent K going to zero at the equator, f is again replaced by $\sqrt{2\beta c_\mathrm{r}}$ in EG as before for VMHS. Note also that it is in principle possible to include horizontal shear (barotropic) instability in addition to baroclinic instability in the new closure (Eden and Greatbatch, 2008b), which is however not considered in the present study.

3. Results

3.1. Thickness diffusivity in the simulations

In this section, we compare the simulated values of the thickness diffusivity K in our main experiments. We first note that a priori knowledge of the magnitude and the vertical and horizontal patterns of thickness diffusivity is hampered by the lack of large-scale coverage of observational estimates for sub-surface eddy statistics. However, quantitative model based estimates of K (Ferreira et al., 2005; Eden et al., 2007; Eden, 2006) agree in the finding that K should be large within western boundary currents and on the northern flank of the Antarctic Circumpolar Current (ACC) and smaller elsewhere. Furthermore, K should be in general large, $\mathcal{O}(1000$ m^2/s), near the surface and rapidly decaying with depth. Here, we discuss how well these features are captured in the experiments. The horizontal distributions of the thickness diffusivity K in the main thermocline in the four basic model simulations are shown in Fig. 1, while the zonally averaged, vertical distributions in the Pacific Ocean are shown in Fig. 2.
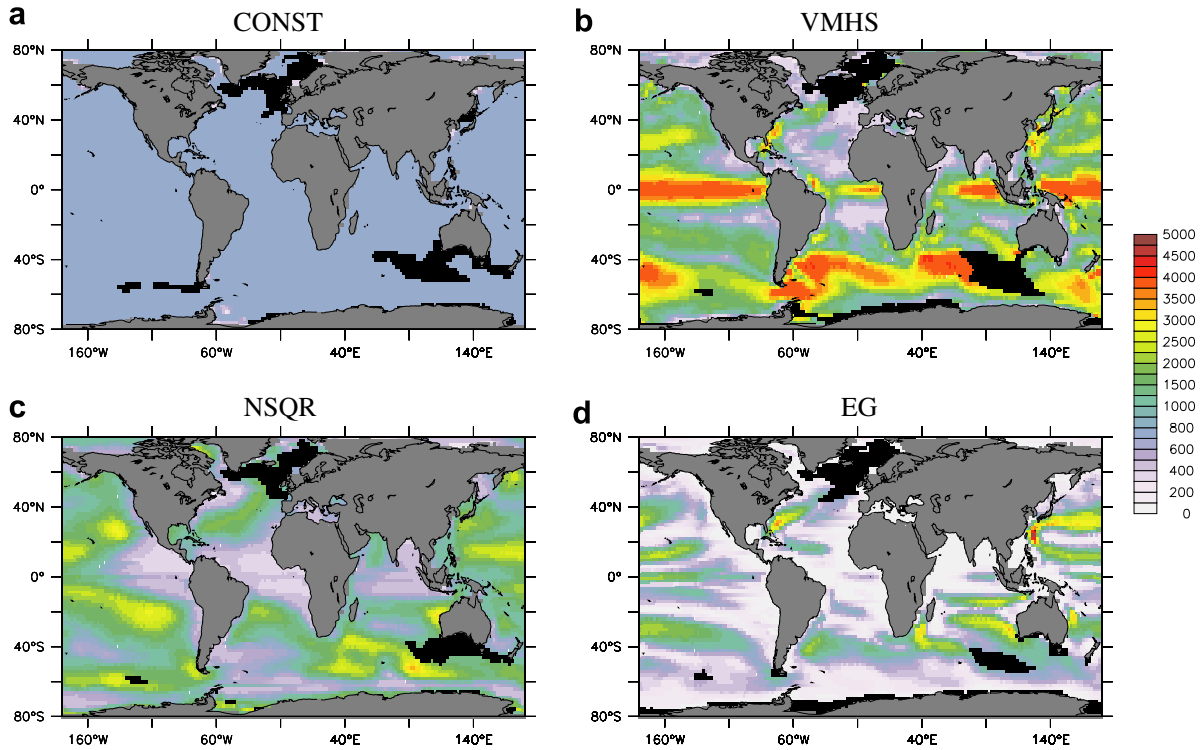
Fig. 1. Annual mean thickness diffusivity (K) in m²/s at 300 m depth in experiment CONST (a), VMHS (b), NSQR (c) and EG (d) after 500 years integration. Values of K are shown for the interior region only, i.e. values of K in the (seasonal maximum) diabatic surface and transition layer are not shown and shaded black. Note the non-linear colour scale for the thickness diffusity. Note also that the data have been interpolated from the model grid to a regular rectangular grid of similar resolution prior to plotting. The land mask in the figure (taken from Smith and Sandwell (1997)) differs therefore slightly from the model's land mask.
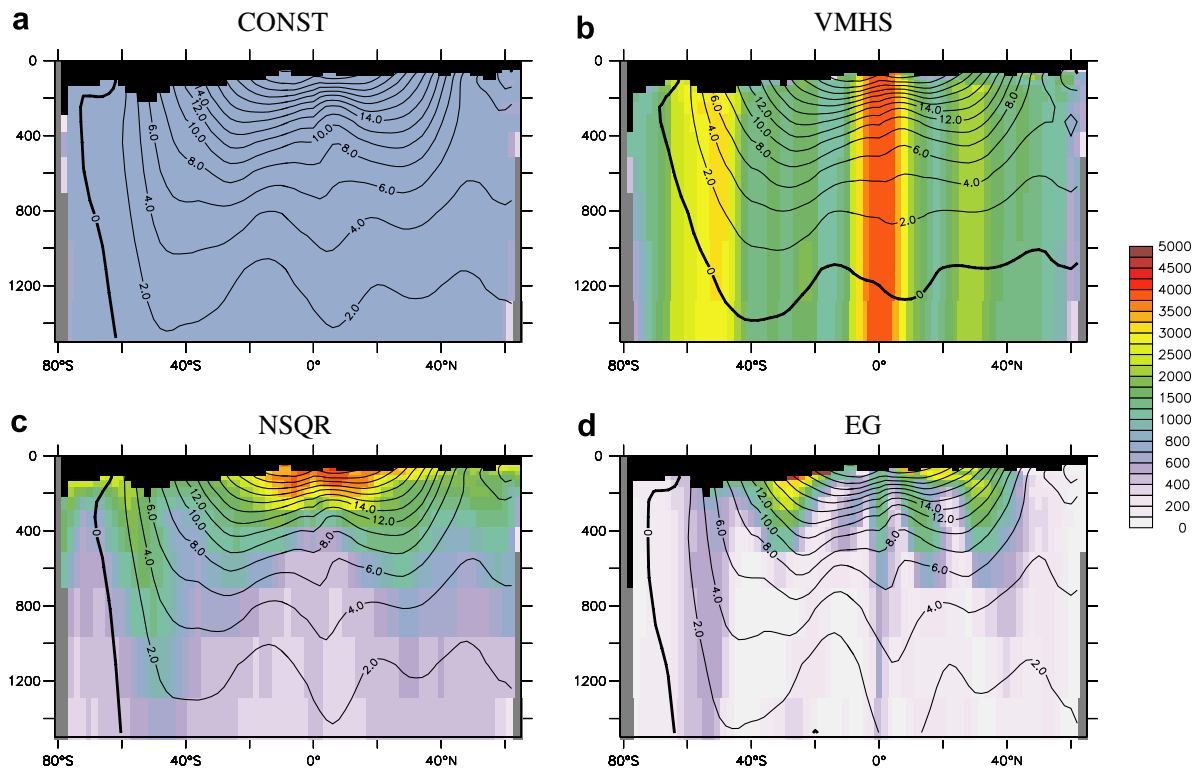

Fig. 2. Annual mean thickness diffusivity (K) in m²/s in the Pacific Ocean in experiment CONST (a), VMHS (b), NSQR (c) and EG (d) after 500 years integration. Shown is the zonally averaged K between 140°E and 120°W (shading) and contour lines of the zonally averaged temperature (2 °C contour interval). Values of K in the (seasonal maximum) diabatic surface and transition layer are not shown (shaded black), such that the zonal average shows K only below the zonally and seasonally maximum mixed layer depth.

In experiment CONST the effect of the tapering scheme of Ferrari et al. (in press) can be seen, which becomes active in the polar regions where deep mixed layers are seen, near lateral boundaries and in a relatively thin near surface layer. Note that this tapering scheme is identical for all experiments. In VMHS, K is large, up to the upper bound of 4000 m^2/s near the equator, in the Southern Ocean and in the western boundary currents but vertically constant below the diabatic layer near the surface. Since the length scale L in VMHS is given by the local grid spacing Δ, except for the tropics where the Rossby radius $\bar{L}_r$ becomes larger than Δ, the horizontal structure at higher latitudes depends to a large degree on the mean Eady growth rate $\bar{\sigma}$ (the effect of the reduced grid spacing in K towards the poles is minor). The maximum in K near the equator can be explained by the large $\bar{L}_r$ while all remaining maxima of K in VMHS, i. e. in the Southern Ocean and in the western boundary currents, coincide with maxima in $\bar{\sigma}$. Therefore, maxima in off-equatorial values of K in VMHS are related to maxima in horizontal buoyancy gradients and vertical shears associated with the ACC and the western boundary currents.

In experiment NSQR, values of K in the main thermocline are in general smaller than in VMHS, but note that they reach $K = 4000$ m^2/s at each water column at the base of the surface diabatic layer by construction. As expected K is large near the surface and decreases with depth. In regions of strong near surface stratification, such as in the tropical Pacific with its sharp thermocline, K shows a faster decay with depth compared to regions where the stratification varies less with depth, as e.g. in the Southern Ocean. The result is large values of K in the near surface Pacific, comparable to VMHS, and moderate values in the Southern Ocean.

In experiment EG, K is large where large horizontal density gradients and vertical shears can be found. This is similar to VMHS, with however smaller values of K in the Southern Ocean and the tropics due to the smaller length scale L. Note that L becomes the Rhines scale L_{Rhi} equatorwards of about 30° latitude (and in regions of very weak eddy energy), otherwise L is the local Rossby radius as discussed in Eden and Greatbatch (2008b) and Eden (2007). The vertical structure of K in EG is similar to NSQR, but note that the horizontal maxima of K in NSQR differ from EG. In NSQR, maxima can be found in the centre of the subtropical gyres, which is in particular evident for the North Atlantic, while in EG the maxima are near the western boundary currents and in regions of strong isopycnal slopes.

3.2. Impact of the thickness diffusivity on the model biases

The changes in thickness diffusivities in the individual experiments produce in turn in differences in the simulated watermasses and circulation. We first note that in all experiments large
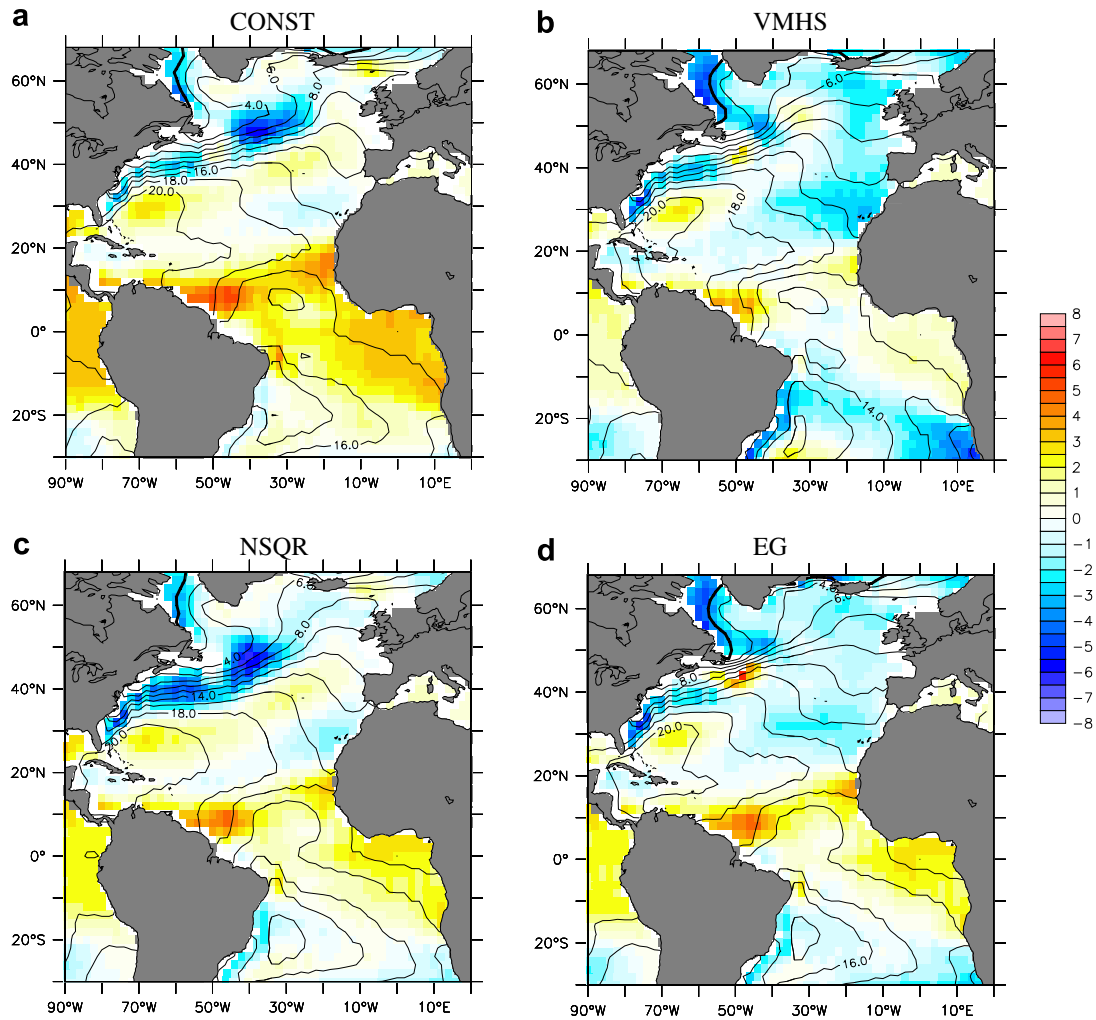

Fig. 3. Annual mean temperature difference between simulation and the climatology of Levitus and Boyer (1994) in experiment CONST (a), VMHS (b), NSQR (c) and EG (d) after 500 years integration at 200 m depth. Also shown are contour lines of temperature (2 °C contour spacing). Note that the data have been interpolated from the model grid to a regular rectangular grid of similar resolution prior to plotting. The land mask in the figure (taken from Smith and Sandwell (1997)) differs therefore slightly from the model's land mask.

temperature biases up to 8 °C can be found, in particular in regions of strong lateral or vertical temperature gradients, when compared to observational estimates of Levitus and Boyer (1994). Biases of similar relative magnitude (with respect on their effect on density) can be seen in the salinity distribution of the simulations. Although the magnitudes and spatial distributions of these model biases change and sometimes decrease by adjusting the thickness diffusivity in the individual experiments, in none of the simulations the temperature and salinity biases are reduced to a value well below the observational error margin and all simulations still remain significantly biased.

We discuss in this section five exemplary climatological aspects of the simulations from which we try to assess their performance. These aspects are the western boundary current system in the North Atlantic, the equatorial thermocline, the North Atlantic meridional overturning and gyre strength, ventilation of the North Atlantic and the meridional overturning and zonal current strength in the Southern Ocean.

3.2.1. Western boundary current system of the North Atlantic

Fig. 3 shows a prominent example of a typical model bias, related to the missing Northwest Corner of the North Atlantic Current (NAC) which often comes along with a displaced Gulf Stream. This well-known artifact shows up in many coarse resolution ocean models and vanishes sometimes when going to much higher horizontal resolution (Smith et al., 2000; Chassignet and Garraffo, 2001). It leaves its imprint in a large negative temperature bias in the subpolar North Atlantic in experiment CONST. This bias is still present in experiment NSQR but decreases much in experiment EG and VMHS. In fact, the negative temperature bias east of Newfoundland of up to 5 °C in experiment CONST and NSQR almost vanishes in EG and VMHS. Furthermore, small region with a positive bias appears east of Newfoundland. The average rms temperature biases between 40° and 60°N at 200 m depth in the North Atlantic are 2 °C, 1.8 °C, 2.2 °C and 1.7 °C for CONST, VMHS, NSQR and EG, respectively. It is clear that the diminishing negative temperature bias in EG and VMHS is related to a different pathway of the Gulf Stream and the NAC around Newfoundland and the interior subpolar gyre. Note that this pathway determines to a large extent the subpolar front in the North Atlantic and is in better

agreement with the observed paths in experiment EG and VMHS compared to the other experiments.

Fig. 4 shows a meridional section of the temperature biases and zonal velocity within the upper thermocline of the North Atlantic, showing that the core of the NAC is indeed displaced southward by several hundred km in CONST and NSQR compared to the other experiments. The negative temperature bias due to the southward displacement of the NAC in CONST and NSQR extends down to almost 1000 m depth. The average rms temperature biases for the region shown in Fig. 4 are 1.5 °C, 2.4 °C, 1.8 °C and 1.2 °C for CONST, VMHS, NSQR and EG, respectively. In VMHS, the NAC is much weaker compared to EG, and a larger negative temperature bias shows up below the main thermocline in the subtropical gyre. These artifacts in VMHS can be attributed to the presence of large values of K which do not decay with depth (as in EG). Note, however, that the horizontal near surface structure of K is similar in VMHS and EG in the North Atlantic (Fig. 1), leading to the improvement with respect to the path of the NAC in both experiments.

3.2.2. Equatorial thermocline

Fig. 3 shows that there are also large temperature biases in the tropical Atlantic when compared with the climatology of Levitus and Boyer (1994). They are largely positive in CONST, NSQR and EG and slightly smaller in VMHS (at 200 m depth). This comes along with a sharper and shallower equatorial thermocline in VMHS. Fig. 5 shows a zonal section of the temperature biases from all cases along the equator. The largest differences between cases can be found below about 150 m depth. A too deep equatorial thermocline can be seen in the Indian and Atlantic Ocean in CONST, NSQR and EG, while in VMHS this bias is reduced. In the Pacific Ocean, a similar improvement is seen in VMHS while CONST has the largest positive biases between 100 and 300 m depth. The larger (and vertically constant) thickness diffusivity in VMHS compared to the other experiments apparently reduces the temperature bias in the equatorial ocean by lifting the thermocline but results in the largest negative biases below 400 m depth amongst all cases.

3.2.3. North Atlantic meridional overturning and gyre circulation

The relative changes in the simulated circulation are in general small. Exceptions are changes in the western boundary currents of
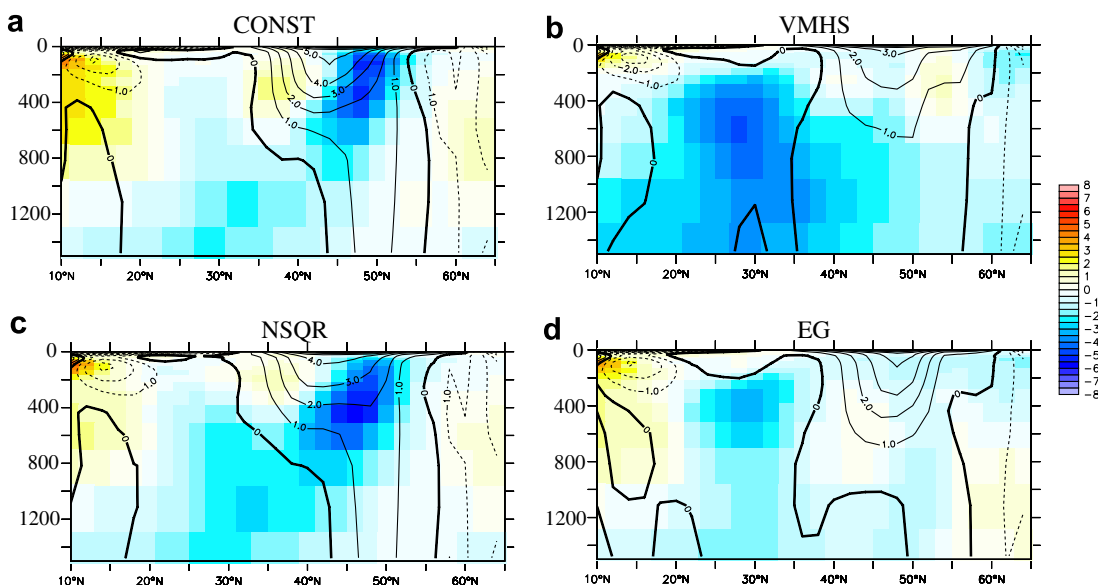

Fig. 4. Annual mean temperature difference between simulation and the climatology of Levitus and Boyer (1994) in experiment CONST (a), VMHS (b), NSQR (c) and EG (d) after 500 years integration as average between 40° and 30°W. Also shown are isolines of annual mean zonal velocity (1 cm/s contour spacing).
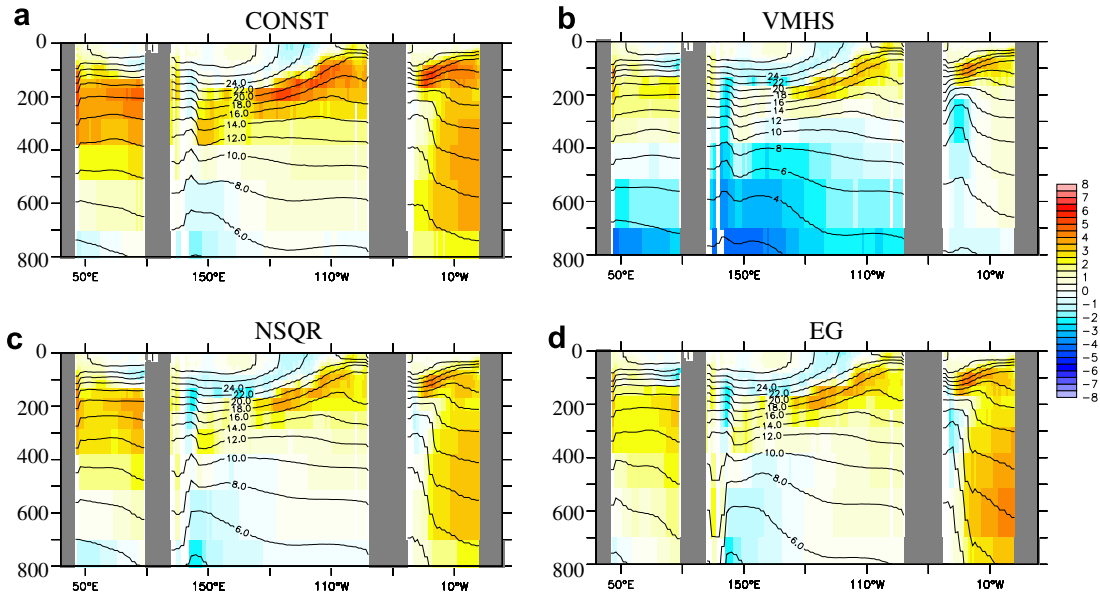
Fig. 5. Annual mean temperature difference between simulation and the climatology of Levitus and Boyer (1994) in experiment CONST (a), VMHS (b), NSQR (c) and EG (d) after 500 years integration at the equator. Also shown are contour lines of temperature (2 °C contour spacing).

the North Atlantic in experiment EG related to the temperature bias in that region as discussed above and changes in the Southern Ocean in VMHS (see below). The maximum strengths of the Eulerian mean meridional overturning circulation (MOC) between 0°N and 70°N in the Atlantic Ocean shown in Fig. 6 are 14.8, 15.2, 9.9 and 11.1 *Sv* for experiments CONST, NSQR, VMHS and EG, respectively. The values for VMHS and EG appear low biased when compared with observational estimates of the MOC in the North Atlantic which range between $15 \pm 2Sv$ (Ganachaud and Wunsch, 2000) and $18 \pm 5Sv$ (Talley et al., 2003). Eddy-resolving models of the North Atlantic also show higher values for the MOC (Smith et al., 2000; Eden and Böning, 2002). Note also that

the vertical structure of the deep overturning cell in the North Atlantic is different in VMHS compared to the other experiments.

The case-to-case differences in the western boundary currents of the North Atlantic as discussed in Section 3.2.1 are also associated with substantial changes in the horizontal gyre circulations. The maximum transports of the subtropical (subpolar) gyre in the North Atlantic (not shown) are 31.1, 32.0, 31.9 and 26.3 *Sv* (31.3, 32.1, 23.6 and 13.7 *Sv*) for experiments CONST, NSQR, VMHS and EG, respectively. It is clear that the horizontal gyre strengths, in particular the strength of the subpolar gyre, are significantly smaller in experiment EG compared to the other experiments. However, note that the subpolar gyre strength in all experiments
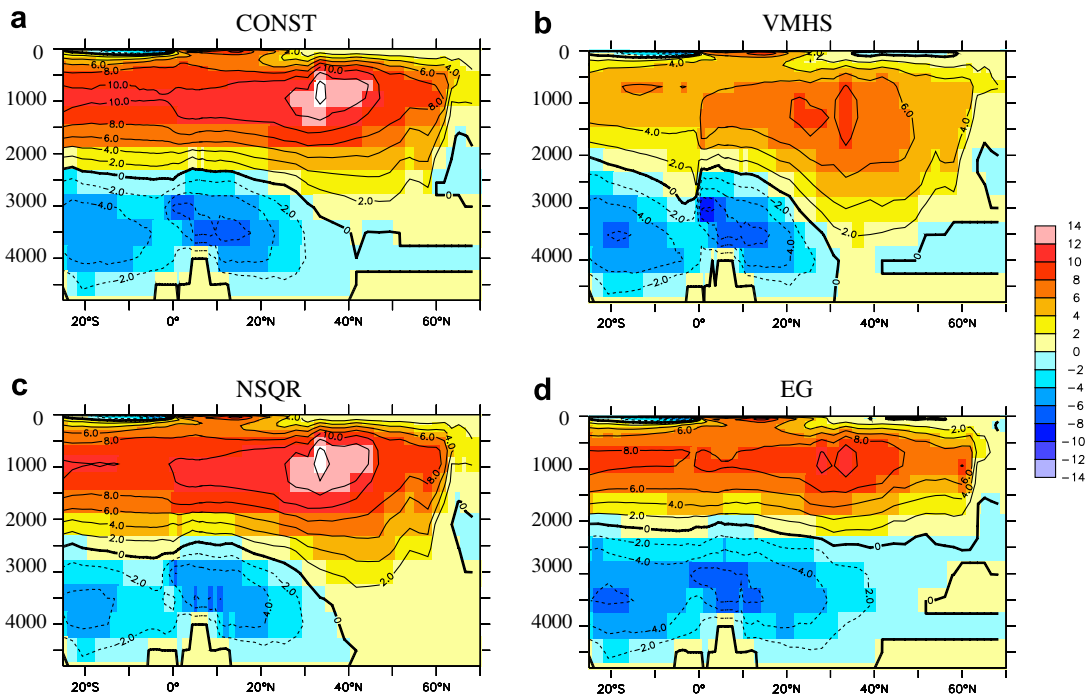

Fig. 6. Annual mean meridional overturning streamfunction in experiment CONST (a), VMHS (b), NSQR (c) and EG (d) after 500 years integration in *Sv* in the Atlantic Ocean. Shown is the streamfunction for the Eulerian mean advection velocity.

is also significantly lower than the observational estimates of around 40 Sv (Pickart et al., 2002). Furthermore, none of the experiments show the observed strong recirculations cells in the Gulf Stream region with transports exceeding 100 Sv (Johns et al., 1995) such that the subtropical gyre strength appears also drastically underestimated by each experiment. The dependency of the subtropical and subpolar gyre strength on the value of K is explored below in more detail in Section 3.3.

3.2.4. North Atlantic ventilation rates

To compare ventilation rates among the experiments, a standard ideal age tracer τ was integrated simultaneously during the model simulations. The source function for τ is given by one unit per model year. Fig. 7 shows τ in the lower limb of the MOC in the North Atlantic after 500 years of model integration. It is clear that the ventilation of the deep North Atlantic appears to be strongest in EG despite is its low MOC. Furthermore, the ideal age of the watermasses within the deep western boundary current is significantly younger and more concentrated at the western boundary in experiment EG compared to the other experiments. However, the different model results are difficult to interpret because of lack of observational data. Note that mixing of watermasses with different concentrations typically biases age estimates from transient tracers like CFCs or ^{14}C toward younger values, such that those sources of information have to be interpreted carefully. On the other hand, all our experiments are with respect to watermass age in the range of model results reported from model intercomparison projects (Dutay et al., 2002).

The younger North Atlantic deep waters in EG appear to be in turn related to the depth of deep convection in the Labrador Sea: maximum mixed layer depths in CONST, NSQR and VMHS are not deeper than 1500 m, while in EG the winter time convection reaches depths of greater than 2000 m in the central Labrador Sea. In VMHS, we find the weakest ventilation of the subpolar North Atlantic coinciding with the shallowest mixed layer depths. Note that the shallow mixed layer depth of less than 1000 m in VMHS appears inconsistent with observations (Pickart et al., 2002) (although deep convection show strong interannual variability in the Labrador Sea hampering the direct comparison with our climatological simulations) while the other experiments seem to be consistent with the observations in this respect.

Note that we find strongest gradients in ventilation age in the deep, western North Atlantic for experiment EG, weaker gradients in CONST and NSQR and even weaker ones in VMHS as a consequence of using different isopycnal diffusivities in the experiments. Note also that the deep flow appears to be detached from the coastline of the subtropical North Atlantic in VMHS, inconsistent with observations of a continuous deep western boundary current south of the Gulf Stream separation (Lee et al., 1996).
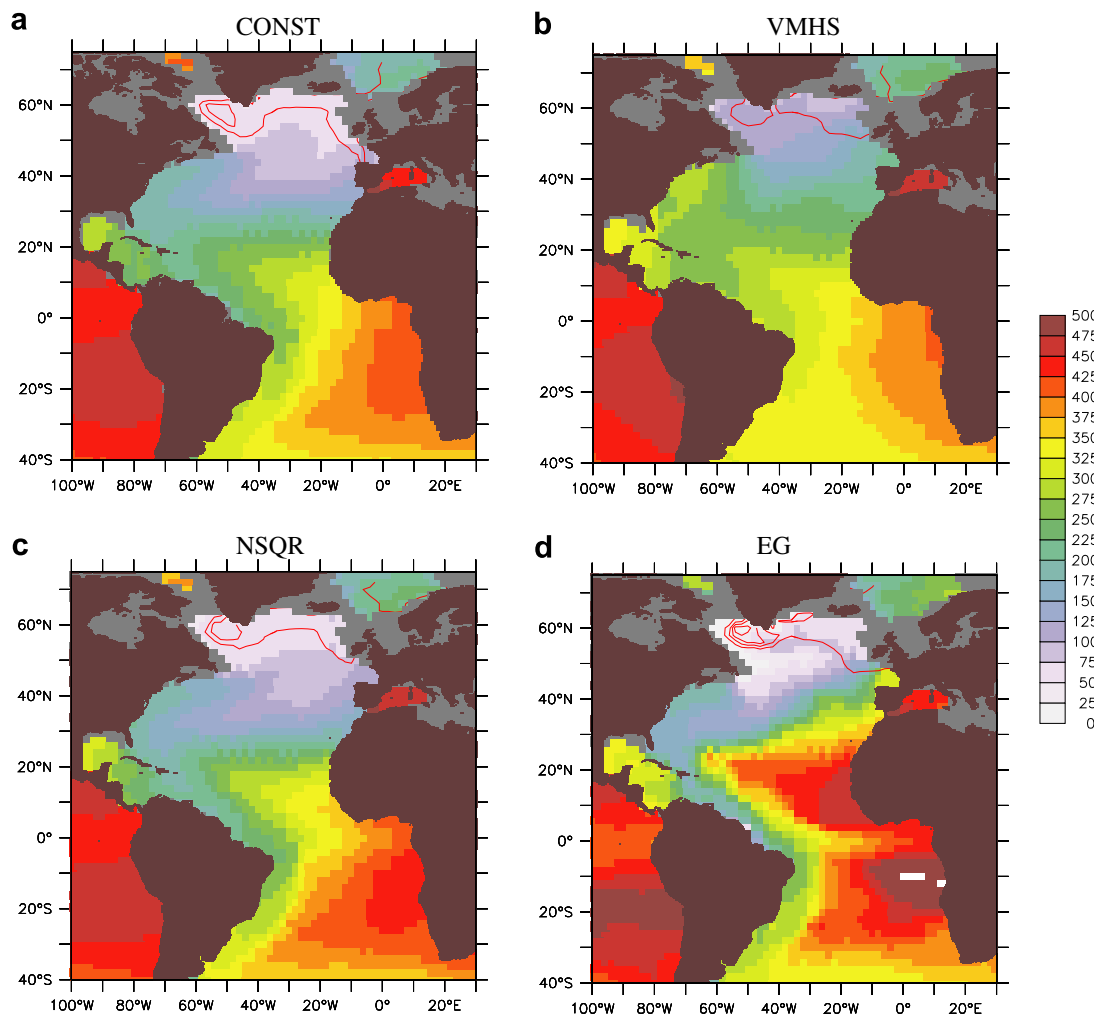

Fig. 7. Ideal age tracer τ in experiment CONST (a), VMHS (b), NSQR (c) and EG (d) after 500 years integration in *years* (shading). Shown is the vertical average of the annual mean τ between 1500 and 2500 m depth. Also shown are isolines (red lines) of the maximum mixed layer depth in the individual experiments with 500 m contour spacing. Note that the data have been interpolated from the model grid to a regular rectangular grid of similar resolution prior to plotting. The land mask in the figure (taken from Smith and Sandwell (1997)) differs therefore slightly from the model's land mask.

3.2.5. Overturning and zonal current strength in the Southern Ocean

The ACC transport depends not only on surface forcing, stratification and bottom topography (Olbers et al., 2006) but also on thickness diffusion (Danabasoglu and McWilliams, 1995) and other subgrid-scale parameters, such as viscosity (Jochum et al., 2008). In particular, increasing thickness diffusion leads to a reduced ACC transport. The observational estimate of the transport through the Drake Passage between Antarctica and South America is 134 ± 13 Sv (Whitworth and Peterson, 1985). It is the lowest in experiment VMHS, only 71.7 Sv, and higher, i.e. 133.1, 143.8 and 140.6 Sv in the experiments CONST, NSQR and EG, respectively. The dependency of the ACC transport on K (larger transport for smaller K, compare also Fig. 1) is consistent with the previously found sensitivity.

The low bias in ACC transport in VMHS is accompanied by a large change in the MOC of the Southern Ocean compared to the other cases. Fig. 8 shows the total MOC, i.e. Eulerian mean plus transient eddy contribution (parameterised by the thickness diffusivity) in each experiment (note that the standing eddy contribution is not shown but will also contribute to the residual streamfunction for zonal mean tracer). While in experiments CONST, NSQR and EG a meridional circulation of similar strength and familiar structure shows up, the circulation in the upper 2000 m in experiment VMHS is rather different from the other experiments coming along with the larger thickness diffusivity in the Southern Ocean. In fact, the near surface equatorwards transport between 65° and 45°S has almost vanished in VMHS. On the other hand, the structure of the MOC in the Southern Ocean is not well constrained from observations, such that we cannot interpret the results of VMHS in this respect as a further model bias.

3.3. Dependency on parameters

In this section, we investigate further the sensitivity of the model solutions to the value of K. Using additional model experiments with different choices for the parameter α in VMHS and the parameters c and γ in EG, we document changes in the equatorial thermocline depth, the temperature biases due to the missing Northwest Corner of the NAC, and the North Atlantic subpolar gyre strength. Each additional experiment is integrated for 100 years, which we consider to be sufficient to capture the bulk of the sensitivities and to assess the differences between the individual experiments.

3.3.1. Parameter α in VMHS

In VMHS, the smaller ACC transport is related to the large values of the thickness diffusivity in the Southern Ocean. We have reduced K by lowering the parameter α from $\alpha = 0.13$ to $\alpha = 0.04$ in a further experiment denoted as VMHS_LOW. The resulting K in the main thermocline is shown in Fig. 9a). The change in thickness diffusivity yields a higher Drake passage transport of 103.6 Sv, in better agreement to the observational estimates, although still too low compared to the observational estimates, such that one might tend to reduce α even further. On the other hand, we notice that the thickness diffusivities in the North Atlantic are now also much lower in VMHS_LOW compared to VMHS and all other experiments. Note that K in VMHS_LOW comes in fact close to the large-scale pattern of K in Wright (1997) who uses the width of the baroclinic zone as length scale in VMHS.

The reduced K in the North Atlantic is related to an increased cold temperature bias related to a missing Northwest corner and a southward displacement of the NAC (Fig. 9b). Since K in VMHS_LOW is also smaller in the tropical Atlantic compared to VMHS, the bias of a too deep equatorial thermocline is further enhanced. We conclude that by tuning the single parameter α it appears impossible to improve the parameterisation of K and the model simulation at all locations at the same time. In order to reduce all biases one would have to use a different length scale L or a different time scale σ^{-1} in VMHS (or a spatially dependent parameter α which would be equivalent). We also note that better results would be obtained in VMHS using the length scale proposed in Eden and Greatbatch (2008b).
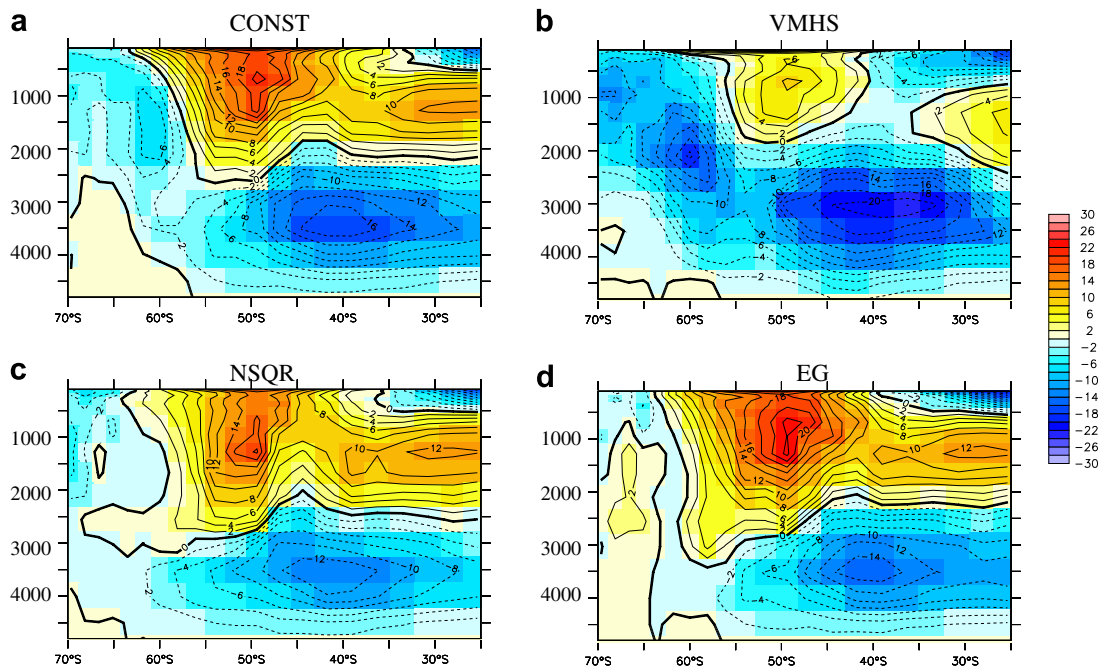

Fig. 8. Annual mean meridional overturning streamfunction in experiment CONST (a), VMHS (b), NSQR (c) and EG (d) after 500 years integration in Sv in the Southern Ocean. Shown is the streamfunction for the total tracer advection velocity, i.e. the Eulerian mean velocity plus the transient eddy contribution given by the parameterised bolus velocities.
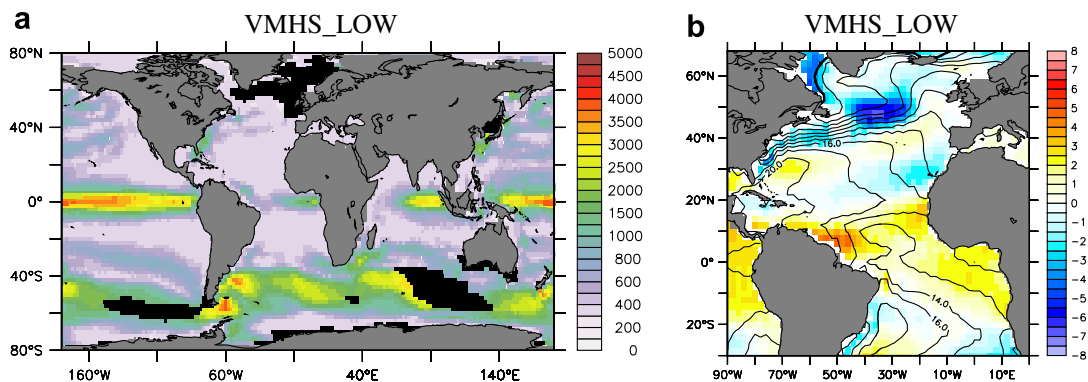
Fig. 9. (a) Annual mean thickness diffusivity (K) in m^2/s at 300 m depth in experiment VMHS_LOW after 100 years integration. Values of K are shown for the interior region only, i.e. values of K in the (seasonal maximum) diabatic surface and transition layer are not shown and shaded black. (b) Annual mean temperature difference between VMHS_LOW and the climatology of Levitus and Boyer (1994) at 200 m depth. Also shown are contour lines of temperature (2 °C contour spacing). Note that the data have been interpolated from the model grid to a regular rectangular grid of similar resolution prior to plotting. The land mask in the figure (taken from Smith and Sandwell (1997)) differs therefore slightly from the model's land mask.

3.3.2. Parameter c in EG

In experiment EG, the thickness diffusivity is given by $K = cL^2\sigma$. The effect of a smaller or larger value of the parameter c, yielding smaller or larger values of K, is consistent with the previous discussed effects of the value of K on the circulation. Changing c from $c = 2$ in EG to $c = 1$ in the sensitivity experiment EG_LOW (to $c = 3$ in the experiment EG_HIGH), the Drake passage transport after 100 years of integration is increased (decreased) from 151.2 to 170.3 Sv (139.6 Sv). The strength of the subtropical gyre in the North Atlantic decreases from 28.4 Sv in EG_HIGH to 25.3 Sv in EG, but stays almost constant at 25.6 Sv in EG_LOW when further reducing c going from EG to EG_LOW. The subpolar gyre strength decreases from 16.1 Sv in EG_HIGH to 14.0 Sv in EG and 12.6 Sv in EG_LOW. However, the maximum mixed layer depth in the Labrador Sea and the ideal age in EG, EG_HIGH and EG_LOW remains very similar.

The substantial reduction of the cold bias in the North Atlantic in EG is very similar in EG_LOW and EG_HIGH (not shown), i.e. the pathway of the NAC appears rather insensitive to the magnitude of K. In contrast, the equatorial thermocline depth shows a significant sensitivity on c (Fig. 10). For higher (lower) K in the tropical ocean, the equatorial thermocline gets shallower (deeper). In fact, the temperature in EG_HIGH is now in good agreement below approximately 200 m in the tropical Pacific and Indian Ocean, although the tropical Atlantic still shows a warm bias below the thermocline. Consistently, the equatorial temperature biases are getting larger in EG_LOW.

Note that the dependency of the subpolar gyre strength on K is also consistent with NSQR and VMHS: Here, K is larger in both experiments NSQR and VMHS since lower bounds for K have been prescribed in both, which we have not done in EG, EG_LOW and EG_HIGH. Thus, larger subpolar gyre strengths correspond to high-

er values of K. To test the influence of a lower bound of K on the circulation in the sensitivity experiment EG_BOUND we have employed the lower bound $K \geqslant 300$ m^2/s on the thickness diffusivity. In EG_BOUND, the Drake passage transport stays almost the same as in EG, while the subpolar (subtropical) gyre strength in the North Atlantic increases after 100 years of integration from 14.0 (25.4) Sv in EG to 17.2 (26.0) Sv in EG_BOUND. We also notice that maximum convection depth in the Labrador Sea and the ventilation rates as simulated by the ideal age tracer are reduced in EG_BOUND compared to EG. In contrast, the temperature distribution in the upper North Atlantic was almost unchanged in EG_BOUND compared to EG.

3.3.3. Parameter γ in EG

Finally we have assessed the sensitivity to the parameter γ by changing it from $\gamma = 200$ in EG_HIGH to $\gamma = 50$ in EG_GAMMA. As expected, the differences in the simulations are only very small. However, when γ is further reduced to $\gamma = 1$, maximum values of K get too large in regions where the stratification becomes almost zero and a stable integration becomes impossible. This behaviour could of course be omitted by simply employing an upper bound for K (as in the other experiments).

4. Summary and discussion

We have described the effects of different closures for the thickness diffusivity K appropriate for the Gent and McWilliams (1990) parameterisation in a coarse resolution general circulation model of the global ocean. Our choices for K include a constant value (CONST), a variant of the Visbeck et al. (1997) parameterisation (VMHS), a value dependent on the buoyancy frequency N
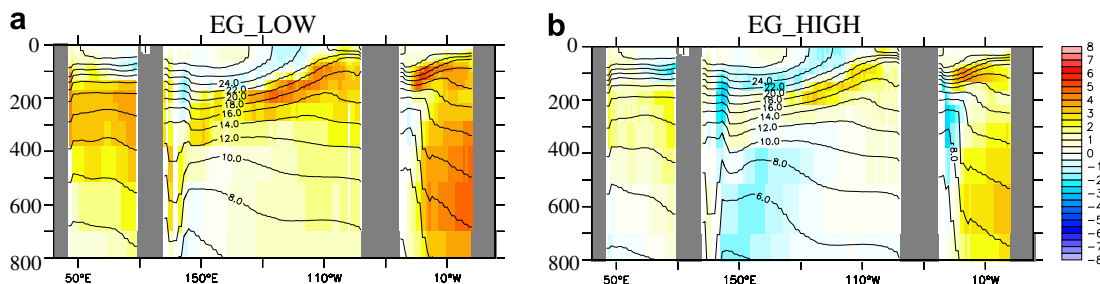

Fig. 10. Annual mean temperature difference between simulation and the climatology of Levitus and Boyer (1994) in experiment EG_LOW (a) and EG_HIGH (b) after 100 years integration at the equator. Also shown are contour lines of temperature (2 °C contour spacing).

(Danabasoglu and Marshall, 2007) (NSQR) and a new closure by Eden and Greatbatch (2008b) (EG). The thickness diffusivity K in VMHS is horizontally varying but constant in the vertical and it is proportional to the local Eady growth rate representative for the main thermocline. The vertical profile of K in NSQR is proportional to the local N^2 profile while no explicit horizontal structure was prescribed. K in EG is both horizontally and vertically varying, proportional to the local Eady growth rate and the square of an eddy length scale given by the minimum of Rossby radius and Rhines scale. In all experiments, the isopycnal diffusivity is specified identical to the thickness diffusivity.

In general, the comparison and evaluation of the simulated thickness diffusivity in the individual experiments are hampered by the lack of large-scale coverage of observational estimates for sub-surface eddy statistics. However, quantitative model based estimates of K (Ferreira et al., 2005; Eden et al., 2007; Eden, 2006) agree in the finding that K should be large within western boundary currents and on the northern flank of the ACC and smaller elsewhere. Furthermore, K should be in general large, $\mathcal{O}(1000\ m^2/s)$, near the surface and rapidly decay with depth. The latter requirement is satisfied for the case in experiments NSQR and EG but not in VMHS and CONST. On the other hand, the former requirement is qualitatively met by all experiments with spatially varying K, although there are relatively large variations in the relative magnitudes of K. In particular, the horizontal distribution of K in NSQR shows elevated values, in fact even maxima, within the centre of the subtropical gyres instead of the western flanks in both the Atlantic and Pacific Oceans and in both hemispheres (see Fig. 1b).

In VMHS, using our choice of the eddy length scale, effectively a constant in off-equatorial regions but decreasing with latitude with the grid spacing, the thickness diffusivity is excessively high in the Southern Ocean or, when "tuning" the parameterisation by lowering the parameter α, too small in the mid-latitude western boundary regions. However, our choice was an attempt to obtain an acceptable fit to the *a priori* knowledge about the lateral distribution of K using a combination of the eddy length scales proposed by Visbeck et al. (1997). Using just the local Rossby radius as the length scale in VMHS yields too low values of K at higher latitudes, or, in turn, too high values in the subtropics (by adjusting the parameter α). Using the width of the baroclinic zone as the eddy length scale yields high values in the Southern Ocean and too small values elsewhere (Wright, 1997). We found it difficult to obtain realistic values of K at all locations at the same time in agreement to our *a priori* knowledge about the lateral distribution of K using the length scale proposed by Visbeck et al. (1997). Better results can be obtained using the length scale proposed by Eden and Greatbatch (2008b). Regardless, we stress that a vertically constant K as in VMHS is not in agreement with our *a priori* knowledge of K.

The changes in K affect the simulated watermass characteristics in a relatively weak but systematic manner. Although none of the experiments are unbiased in temperature (or salinity), we noticed improvements in the near surface North Atlantic and in the equatorial thermocline in some of the experiments. In all sensitivity experiments with the new closure in EG, the pathway of the Gulf Stream and the NAC was more realistic and the negative temperature bias near the subpolar front due to the missing Northwest Corner of the NAC was reduced with potentially positive effects on a coupled model simulation as recently discussed by Weese and Bryan (2006) for the CCSM climate model.

Since this important improvement was insensitive to the choice of parameters in EG, i.e. almost identical in EG_LOW, EG_HIGH and EG_BOUND, it might therefore be related to the detailed horizontal structure of K in the North Atlantic, i.e. high within the Gulf Stream/NAC system and low outside those currents. In experiment EG and in VMHS the horizontal structure of the simulated thickness diffusivity in the North Atlantic is similar and agrees better with our *a priori* knowledge of K compared to NSQR, which shows maxima of K in the centre of the subtropical gyre. It should be pointed out, though, that in spite of their different origin, the thermocline structure of EG and NSQR are rather similar, since the vertical structure of the Eady growth rate is similar to the structure of N^2, i.e. large in the thermocline and rapidly decaying below.

A further systematic effect of the magnitude of the thickness diffusivity in the model was the depth of the equatorial thermocline. All experiments agree in the finding that increasing K near the surface of the equatorial ocean lifts the equatorial thermocline. Danabasoglu and Marshall (2007) partly related that effect to increased equatorial upwelling. In addition, a direct effect of the thickness diffusivity can be seen. Fig. 2 illustrates how the Equatorial Undercurrent (EUC), for which the zonal flow is in geostrophic balance at the equator, bends the isotherms at the equator: upwards above the core of the EUC and downwards below it. Compared to CONST, all experiments have an increased thickness diffusivity in the equatorial thermocline. We might speculate that the increased equatorial thickness diffusivity flattens the isotherms there and leads to an equatorial cooling. This lifting and flattening of the thermocline might be welcomed since the model shows a bias of a too deep equatorial thermocline in the reference experiment CONST. However, the improvement of the bias may also come as a surprise, since the physical motivation of the flattening of the isopycnals is based on baroclinic instability theory relevant for mid-latitudes (Gent et al., 1995), while at the equator a different dynamical regime might apply. Therefore, we suggest that the impact of thickness diffusivity on the simulated equatorial dynamics should be viewed with caution. We also note the possibility that the shallower equatorial thermocline is the result of a shoaling subtropical gyre (Pedlosky, 1987; McCreary and Lu, 1994). It is beyond the scope of the present study to decide which of these processes is the dominant. However, since the too deep equatorial thermocline is a long-standing OGCM bias (e.g. Maes et al. (1997)) this connection between thickness diffusion and thermocline depth certainly requires more attention.

In agreement with previous studies, e.g. Danabasoglu and McWilliams (1995), we found that the ACC transport is related to the value of the thickness diffusivity in the model, i. e. larger K lowers the ACC transport. Here we also identified a dependency of the subpolar and subtropical gyre strengths in the North Atlantic to the magnitude of K. A larger K leads to a larger transport both in the subpolar and the subtropical gyres, although the effect is stronger and clearer for the subpolar gyre in the individual experiments. A weaker subpolar gyre was also related to deeper convection depths and larger ventilation rates as indicated by an ideal age tracer.

We speculate that the weaker parameterised eddy heat flux resulting from smaller K leads to deeper convection in the Labrador Sea because of less mixing of buoyant water from the boundary currents into the interior Labrador Sea and thus weaker restratification after convection. The mean circulation, in particular the barotropic flow and consequently the subpolar gyre strength was found to be weaker for deeper convection depth, which could be due to the interaction of the barotropic circulation with the topography in the presence of stratification (JEBAR, i.e. Joint Effect of Baroclinicity and Relief, see e.g. Olbers and Eden (2003)). However, note that this is in contrast to what is known from the response of the subpolar gyre strength to atmospheric forcing variability, where deeper convection depths in years of enhanced buoyancy loss over the Labrador Sea are related to a spinup of the subpolar gyre, which was also interpreted as a consequence of JEBAR (Eden and Willebrand, 2001).

On the other hand, freshwater might also be important. Treguier et al. (2005) demonstrated how the peculiar balance between gyre strength, deep convection and freshwater balance

of the subpolar North Atlantic can lead to large biases even in high-resolution ocean models. The role of the thickness diffusivity for this balance and to what extent the effects of K on the subpolar gyre are specific to the particular model which we have used, remain to be demonstrated. Finally we note the possibility that the choice of the isopycnal diffusivity (here identical to thickness diffusivity) can play a larger role for buoyancy and thus the dynamics of the model than one might expect when changes in watermass characteristics become large (Sijp et al., 2006).

Acknowledgements

References

Bryan, K., Dukowicz, J.K., Smith, R.D., 1999. On the mixing coefficient in the parameterization of bolus velocity. J. Phys. Oceanogr. 29, 2442–2456.

Chassignet, E.P., Garraffo, Z.D., 2001. Viscosity parameterization and the gulf stream separation. In: Müller, P., Henderson, W. (Eds.), From Stirring to Mixing in a Stratified Ocean, volume Proceedings'Aha Huliko'a Hawaiian Winter Workshop. University of Hawaii, pp. 37–41.

Chelton, D.B., deSzoeke, R.A., Schlax, M.G., Naggar, K.E., Siwertz, N., 1998. Geographical variability of the first-baroclinic rossby radius of deformation. J. Phys. Oceanogr. 28, 433–460.

Cox, M.D., 1987. Isopycnal diffusion in a z-coordinate ocean model. Ocean Modell. 74, 1–5.

Danabasoglu, G., 2004. A comparison of global ocean general circulation model solutions obtained with synchronous and accelerated integration methods. Ocean Modell. 7, 323–341.

Danabasoglu, G., Ferrari, R., McWilliams, J.C., 2008. Sensitivity of an ocean general circulation model to a parameterization of near-surface eddy fluxes. J. Climate 21, 1192–1208.

Danabasoglu, G., Large, W.G., Tribbia, J.J., Gent, P.R., Briegleb, B.P., McWilliams, J.C., 2006. Diurnal coupling in the tropical oceans of CCSM3. J. Climate 19, 2347–2365.

Danabasoglu, G., Marshall, J., 2007. Effects of vertical variations of thickness diffusivity in an ocean general circulation model. Ocean Modell. 18, 122–141. doi:10.1016/j.ocemod.2007.03.006.

Danabasoglu, G., McWilliams, J., 1995. Sensitivity of the global ocean circulation to parameterizations of mesoscale tracer transports. J. Climate 8, 2967–2987.

Drijfhout, S.S., Hazeleger, W., 2001. Eddy mixing of potential vorticity versus thickness in an isopycnic ocean model. J. Phys. Oceanogr. 31 (2), 481–505.

Dukowicz, J., Greatbatch, R., 1999. The bolus velocity in the stochastic theory of ocean turbulent tracer transport. J. Phys. Oceanogr. 29, 2232–2239.

Dutay, J., Bullister, J., Doney, S., Orr, J., Najjar, R., Caldeira, K., Campin, J., Drange, H., Follows, M., Gao, Y., et al., 2002. Evaluation of ocean model ventilation with CFC-11: comparison of 13 global ocean models. Ocean Modell. 4, 89–120.

Eden, C., 2006. Thickness diffusivity in the Antarctic Circumpolar Current. Geophys. Res. Lett. 33 (L11606). doi:10.1029/2006GL026157.

Eden, C., 2007. Eddy length scales in the North Atlantic. J. Geophys. Res. 112 (C06004). doi:10.1029/2006JC003901.

Eden, C., Böning, C.W., 2002. Sources of eddy kinetic energy in the Labrador Sea. J. Phys. Oceanogr. 32 (12), 3346–3363.

Eden, C., Greatbatch, R.J., submitted for publication. A diagnosis of isopycnal mixing by meso-scale eddies. Ocean Modell.

Eden, C., Greatbatch, R.J., 2008b. Towards a mesoscale eddy closure. Ocean Modell. 20, 223–239.

Eden, C., Greatbatch, R.J., Willebrand, J., 2007. A diagnosis of thickness fluxes in an eddy-resolving model. J. Phys. Oceanogr. 37, 727–742.

Eden, C., Willebrand, J., 2001. Mechanism of interannual to decadal variability of the North Atlantic circulation. J. Climate 14 (10), 2266–2280.

Ferrari, R., McWilliams, J.C., Canuto, V.M., Dubovikov, M., in press. Parameterization of eddy fluxes near oceanic boundaries. J. Climate.

Ferreira, D., Marshall, J., 2006. Formulation and implementation of a residual-mean ocean circulation model. Ocean Modell. 13, 86–107.

Ferreira, D., Marshall, J., Heimbach, P., 2005. Estimating eddy stresses by fitting dynamics to observations using a residual-mean ocean circulation model and its adjoint. J. Phys. Oceanogr. 35, 1891–1910.

Ganachaud, A., Wunsch, C., 2000. Improved estimates of global ocean circulation, heat transport and mixing from hydrographic data. Nature 408, 453–457.

Gent, P.R., McWilliams, J.C., 1990. Isopycnal mixing in ocean circulation models. J. Phys. Oceanogr. 20, 150–155.

Gent, P.R., Willebrand, J., McDougall, T.J., McWilliams, J.C., 1995. Parameterizing eddy-induced tracer transports in ocean circulation models. J. Phys. Oceanogr. 25, 463–474.

Green, J.S., 1970. Transfer properties of the large-scale eddies and the general circulation of the atmosphere. Q. J. R. Met. Soc. 96, 157–185.

Griffies, S.M., Gnanadesikan, A., Dixon, K.W., Dunne, J.P., Gerdes, R., Harrison, M.J., Rosati, A., Russell, J.L., Samuels, B.L., Spelman, M.J., Winton, M., Zhang, R., 2005. Formulation of an ocean model for global climate simulations. Ocean Sci. 1, 45–79.

Held, I., Larichev, V., 1996. A scaling theory for horizontally homogeneous, baroclinically unstable flow on a beta plane. J. Atmos. Sci. 53 (7), 946–952.

Jochum, M., 1997. Eine ortsabhängige Parameterisierung von Wirbelflüssen. Master's thesis, Institut für Meereskunde, Kiel.

Jochum, M., Danabasoglu, G., Holland, M., Kwon, Y.-O., Large, W.G., 2008. Ocean viscosity and climate. J. Geophys. Res. 113 (C06017). doi:10.1029/2007JC004515.

Johns, W., Shay, T., Bane, J., Watts, D., 1995. Gulf Stream structure, transport, and recirculation near 68°W. J. Geophys. Res. 100, 817–838.

Large, W.G., Danabasoglu, G., Doney, S.C., McWilliams, J.C., 1997. Sensitivity to surface forcing and boundary layer mixing in a global ocean model: annual-mean climatology. J. Phys. Oceanogr. 27, 2418–2447.

Large, W.G., McWilliams, J.C., Doney, S.C., 1994. Oceanic vertical mixing: a review and a model with a nonlocal boundary layer parameterization. Rev. Geophys. 32, 363–403.

Large, W.G., Yeager, S.G. 2004. Diurnal to decadal global forcing for ocean and sea-ice models: the data sets and flux climatologies. NCAR/TN-460+STR 105 pp., NCAR. Available from: <http://www.cgd.ucar.edu/oce/pubs/04pubs.html>.

Larichev, V., Held, I., 1995. Eddy amplitudes and fluxes in a homogenous model of fully developed baroclinic instability. J. Phys. Oceanogr. 25, 2285–2297.

Ledwell, J.R., Watson, A.J., Law, C.S., 1998. Mixing of a tracer in the pycnocline. J. Geophys. Res. 103 (C10), 21499–21529.

Lee, T.N., Johns, W.E., Zantopp, R.J., Fillenbaum, E.R., 1996. Moored observations of western boundary current variability and thermohaline circulation at 26.5° in the subtropical North Atlantic. J. Phys. Oceanogr. 26, 962–983.

Levitus, S., Boyer, T.P. 1994. World Ocean Atlas 1994. Technical report, NOAA, US Gov. Print. Off., Washington, DC, USA.

Maes, C., Madec, G., Delecluse, P., 1997. Sensitivity of an equatorial Pacific OGCM to the lateral diffusion. J. Phys. Oceanogr. 125, 958–971.

Marshall, J., Shuckburgh, E. Jones, H., Hill, C., in press. Estimates and implications of surface eddy diffusivity in the southern ocean derived from tracer transport. J. Phys. Oceanogr.

McCreary, J., Lu, P., 1994. Interaction between the subtropical and equatorial ocean circulations: the subtropical cell. J. Phys. Oceanogr. 24, 466–497.

Nakamura, M., Chao, Y., 2000. On the eddy isopycnal thickness diffusivity of the Gent-McWilliams subgrid mixing parameterization. J. Climate 13, 502–510.

Olbers, D., Eden, C., 2003. A model with simplified circulation dynamics for a baroclinic ocean with topography. Part I: waves and wind-driven circulations. J. Phys. Oceanogr. 33, 2719–2737.

Olbers, D., Lettmann, K., Timmermann, R., 2006. Six circumpolar currents – on the forcing of the Antarctic Circumpolar Current by wind and mixing. Ocean Dyn. 57, 12–31.

Pedlosky, J., 1987. An inertial theory for the equatorial undercurrent. J. Phys. Oceanogr. 17, 1978–1985.

Pickart, R., Torres, D., Clarke, R., 2002. Hydrography of the Labrador Sea during active convection. J. Phys. Oceanogr. 32, 428–457.

Redi, M.H., 1982. Oceanic isopycnal mixing by coordinate rotation. J. Phys. Oceanogr. 12, 1154–1158.

Rix, N., Willebrand, J., 1996. A note on the parameterisation of eddy-induced mixing from eddy-resolving model data. J. Phys. Oceanogr. 26, 2281–2285.

Roberts, M.J., Marshall, D.P., 2000. On the validity of downgradient eddy closures in ocean models. J. Geophys. Res. 105 (C12), 28.613–28.627.

Sijp, W., Bates, M., England, M., 2006. Can isopycnal mixing control the stability of the thermohaline circulation in ocean climate models? J. Climate 19, 5637–5651.

Smith, R.D., Gent, P.R., 2004. Reference manual for the Parallel Ocean Program (POP): ocean component of the Community Climate System Model (CCSM2.0 and 3.0). Tech. Rep. LA-UR-02-2484 75 pp., Los Alamos National Laboratory, Los Alamos, NM, USA. Available from: <http://www.ccsm.ucar.edu/models/ccsm3.0/pop>.

Smith, R.D., Maltrud, M.E., Bryan, F.O., Hecht, M.W., 2000. Numerical simulation of the North Atlantic Ocean at 1/10°. J. Phys. Oceanogr. 30, 1532–1561.

Smith, W.H.F., Sandwell, D.T., 1997. Global seafloor topography from satellite altimetry and ship depth soundings. Science 277, 1957–1962.

Solovev, M., Stone, P., Malanotte-Rizzoli, P., 2002. Assessment of mesoscale eddy parameterizations for a single-basin coarse-resolution ocean model. J. Geophys. Res. 107 (C9), 1–9. doi:10.1029/2001JC001032.

Stammer, D., 1998. On eddy characteristics, eddy transports, and mean flow properties. J. Phys. Oceanogr. 28 (4), 727–739.

Stone, P.H., 1971. Baroclinic instability under non-hydrostatic conditions. J. Fluid Mech. 45, 659–671.

Stone, P.H., 1972. A simplified radiative-dynamical model for the static stability of rotating atmospheres. J. Atmos. Sci. 29, 405–418.

Talley, L., Reid, J., Robbins, P., 2003. Data-based meridional overturning streamfunctions for the global ocean. J. Climate 16, 3213–3226.

Theiss, J., 2004. Equatorward energy cascade, critical latitude, and the predominance of cyclonic vortices in geostrophic turbulence. J. Phys. Oceanogr. 34, 1663–1678.

Treguier, A., Theetten, S., Chassignet, E., Penduff, T., Smith, R., Talley, L., Beismann, J., Böning, C., 2005. The North Atlantic subpolar gyre in four high-resolution models. J. Phys. Oceanogr. 35 (5), 757–774.

Treguier, A.M., 1999. Evaluating eddy mixing coefficients from eddy-resolving ocean models: a case study. J. Mar. Res. 57, 89–108.

Visbeck, M., Marshall, J., Haine, T., Spall, M., 1997. Specification of eddy transfer coefficients in coarse-resolution ocean circulation models. J. Phys. Oceanogr. 27, 381–402.

Weese, S., Bryan, F., 2006. Climate impacts of systematic errors in the simulation of the path of the North Atlantic Current. Geophys. Res. Lett. 33 (19).

Whitworth, T., Peterson, R.G., 1985. Volume transport of the Antarctic Circumpolar Current from bottom pressure measurements. J. Phys. Oceanogr. 15 (6), 810–816.

Wright, D., 1997. A new eddy mixing parameterization in an ocean general circulation model. International WOCE Newsletter 26, 27–29.

Yeager, S.G., Shields, C.A., Large, W.G., Hack, J.J., 2006. The low resolution CCSM3. J. Climate 19, 2545–2566.

Zhurbas, V., Oh, I.S., 2004. Drifter-derived maps of lateral diffusivity in the Pacific and Atlantic Oceans in relation to surface circulation patterns. J. Geophys. Res. 109 (C05015).